A Data Focusing method for Microwave Imaging of Extended Targets

T. Gholipur[1], M. Nakhkash[2]
[1] *Department of Electrical Engineering and Computer, Yazd University, Yazd, Iran, t_gholipur@stu.yazd.ac.ir*
[2] *Department of Electrical Engineering and Computer, Yazd University, Yazd, Iran, nakhkash@yazd.ac.ir,*
Corresponding author: M. Nakhkash

***Abstract*- This paper presents a data focusing method (DFM) to image extended targets using the multiple signal classification (MUSIC) algorithm. The restriction on the number of transmitter-receiver antennas in a microwave imaging system deteriorates profiling an extended target that comprises many point scatterers. Under such situation, the subspace-based linear inverse scattering methods, like the MUSIC algorithm, fail to image the extended targets. In proposed method, the DFM divides imaging region into several sections and maps the scattered data to each section by applying a linear transformation. Being weakened clutters from other sections, the resultant focused data contains, mostly, the responses of scatterers inside the desired section. In this way, the number of scatterers is reduced comparing to the number of transmitter-receiver antennas and the requirement for the MUSIC is satisfied. Using experimental data, we show that the DFM in conjunction with the MUSIC is successful in microwave imaging of extended targets.**

***Index Term*-** Microwave imaging, MUSIC algorithm, Focusing method, Extended target.

I. INTRODUCTION

Microwave imaging (MI) is used to determine the spatial dielectric profile of an object from the electromagnetic field that the object scatters under illumination from various directions. Among the methods used for the profile reconstruction in an MI system, the MUSIC algorithm is a promising method for quasi real-time imaging [1]-[7]. This algorithm exploits the orthogonality of the signal and noise subspaces by employing singular value decomposition (SVD) of a so-called multi-static response (MSR) matrix. The MUSIC algorithm locates the point scatterers from the peaks of the well-known pseudo spectrum.

In computing the pseudo spectrum, the number of point scatterers is required to be less than the number of transmitters and receivers. If the number of scatterers exceeds that of transmitter-receiver antennas, all singular vectors in the SVD of the MSR define the signal space, i.e. the noise space has no dimensionality to be used for pseudo spectrum generation in the MUSIC. An extended target is a relatively big distributed scatterer, which can be viewed as a collection of many point scatterers [6]-

Manuscript received 11-Sept.-2017 and revised 22-Dec.-2017, *P- ISSN: 2322-4088*
Accepted on 15- Jan.-2018 *E- ISSN: 2322-3936*

[7] and, hence, the requirement for the MUSIC may not be satisfied. The number of transmitter-receiver antennas cannot be increased, arbitrary, to satisfy the MUSIC requirement. This is because there are restrictions on the number of transmitter-receiver antennas in terms of the working frequency, the antenna size and the required radiation power.

This paper introduces a data focusing method (DFM) to solve the above problem. The DFM, initially, divides the imaging region into several small sections and then, using a linear transformation matched to each section, another matrix is obtained from the original MSR matrix. The resultant matrix contains, mostly, the responses of scatterers inside the aimed section, i.e. the yielded matrix is focused on the reflections from that section. Such a method works similar to a spatial matched filter, which weakens the clutter from the scatterers in other sections so as to highlight the signal power of the scatterers within an intended section. Focusing on a section causes the number of interested scatterers is reduced in comparison to the number of transmitter-receiver antennas and the requirement for the MUSIC is satisfied. The image creation for each section can be performed by any subspace-based linear inversion. However, we employ the MUSIC algorithm, since it provides the super-resolution in locating the targets.

Reference [7], also, investigates the application of the MUSIC algorithm for imaging the extended targets. Assuming the number of transmitters and receivers is enough, it is shown that the MUSIC can image an extended target from the original MSR if the dimension of the signal space can be estimated correctly. The imaging procedure in [7] cannot provide good resolution for practical use, where the number of transmitter-receiver antennas cannot be increased arbitrary. This reference, also, proposes an algorithm to estimate the signal dimension. Computer simulations in [7] indicate that although the estimation algorithm works quite satisfactory, it cannot predict the signal dimension for the optimum image resolution.

Using realistic experimental data, we compare the results of applying the MUSIC to the original MSR and the focused MSR. Our comments on the performance of both applications are given in Section V.

II. MATHEMATICAL FRAMEWORK OF MSR MATRIX

The geometry of the imaging problem is given in Fig. 1, where the background medium is assumed to be homogeneous and non-magnetic, and the imaging is performed under the 2D TM incident. The imaging region D, containing a number of small scatterers with the unknown locations $\mathbf{X}_m$, m =1, …, M, is successively irradiated by N_t transmitters and the scattered electric fields are measured by N_r receivers. The imaging is to get the location and, if possible the shape and dielectric properties of the scatterers based on the data measured by the receivers.

From the scalar Helmholtz equation for a 2D problem in the frequency domain, and by adopting the framework of the Foldy-Lax model [8]-[9], one can express the MSR matrix $\mathbf{K}$ as follows [10]

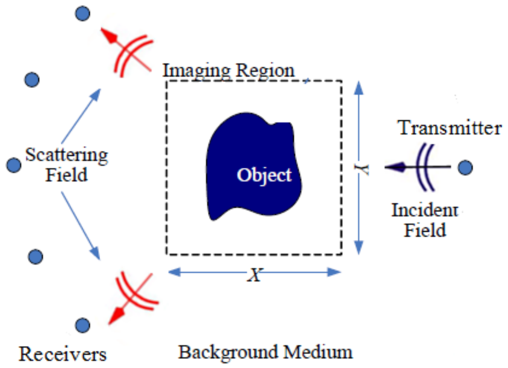

Fig. 1. General setup for a 2D microwave imaging system

$$\mathbf{K} = \sum_{m=1}^{M} \sum_{m'=1}^{M} A_{m,m'} \mathbf{g}_{0,r}(\mathbf{X}_m) \mathbf{g}_{0,t}^{T}(\mathbf{X}_{m'})$$

(1)

where T stands for transposition and $\mathbf{g}_{0,r}(\mathbf{X}_m)$ and $\mathbf{g}_{0,t}(\mathbf{X}_m)$, respectively, are the receive and transmit background Green's function vectors at the target location $\mathbf{X}_m$ that can be written as

$$\mathbf{g}_{0,r}(\mathbf{X}_m) = [G_0(\mathbf{R}_1^r, \mathbf{X}_m), G_0(\mathbf{R}_2^r, \mathbf{X}_m), \ldots, G_0(\mathbf{R}_{N_r}^r, \mathbf{X}_m)]^T$$
$$\mathbf{g}_{0,t}(\mathbf{X}_m) = [G_0(\mathbf{X}_m, \mathbf{R}_1^t), G_0(\mathbf{X}_m, \mathbf{R}_2^t,), \ldots, G_0(\mathbf{X}_m, \mathbf{R}_{N_t}^t)]^T$$

(2)

in which $G_0(\mathbf{r}, \mathbf{r}')$ is the Green's function corresponding to the background medium, $\mathbf{R}_i^r$ and $\mathbf{R}_l^t$ are the position vectors of ith receiver and lth transmitter respectively, $A_{m,m'}$ is multiple scattering amplitudes [10]. It can be seen from (1) that the $N_r \times N_t$ matrix $\mathbf{K}$ can be obtained in terms of only background Green's function vectors and each column of $\mathbf{K}$ corresponds to the scattered field measured at the receiver array due to one active transmitter.

III. MUSIC ALGORITHM

The MSR matrix $\mathbf{K}$ maps the transmitter space to the receiver space, i.e. $\mathbf{C}^{Nt} \rightarrow \mathbf{C}^{Nr}$. The MUSIC method is based on SVD of matrix $\mathbf{K}$. The SVD of $\mathbf{K}$ can be expressed as

$$\mathbf{K} = \sum_{p=1}^{N} \sigma_p \mathbf{u}_p \mathbf{v}_p^{\dagger} \tag{3}$$

where $\sigma_p \geq 0$ are the singular values, $\mathbf{u}_p$ and $\mathbf{v}_p$ are the left and right singular vectors, respectively, $N = \min(N_t, N_r)$ and † denotes the Hermitian. Note that $\sigma_p > 0$ is related to the signal subspace and $\sigma_p = 0$ is related to the null subspace. Using the orthogonality of signal and noise subspaces, sorting the singular values downwards and arranging their associated singular vectors in terms of sorted results, the pseudo spectrum can be calculated as follows

$$P_{r,t}(\mathbf{X}) = \frac{1}{\sum_{p=M+1}^{N} \left|\mathbf{u}_p^{\dagger}\ \mathbf{g}_{0,r}(\mathbf{X})\right|^2 + \sum_{p=M+1}^{N} \left|\mathbf{v}_p^{\dagger}\ \mathbf{g}_{0,t}^{*}(\mathbf{X})\right|^2}$$

(4)

IV. THE DATA FOCUSING METHOD

As understand from (4), the pseudo spectrum cannot be constructed, if $M \geq \min(N_t, N_r)$. When $M < \min(N_t, N_r)$, assigning the large singular values and their associated singular vectors to the signal space and the rest to the noise space, we can generate a pseudo spectrum that locates the dominant scatterers. The number of transmitters and receivers, therefore, must be more than point scatterers so that the MUSIC can be implemented. An extended target can be viewed as a collection of many point scatterers [6]-[7], whose number, practically, exceeds the number of transmitters and receivers, i.e. $M \geq \min(N_t, N_r)$ and the requirement for the MUSIC implementation is not satisfied. In [7], it is assumed that the number of transmitters and receivers can be increased, arbitrary, to satisfy the MUSIC requirement. However, this is not the case for practical applications as there are restrictions imposed by the working frequency, the antenna size and the required radiation power.

The DFM alleviates the above problem by dividing the imaging region into several sections. Letting C_d denote the dth section, two matrices $\mathbf{A}_d$ and $\mathbf{B}_d$ are obtained for this section as:

$$\mathbf{A}_d = [\bar{\mathbf{g}}_{0,t}(\mathbf{X}_{d_1}), \bar{\mathbf{g}}_{0,t}(\mathbf{X}_{d_2}), ..., \bar{\mathbf{g}}_{0,t}(\mathbf{X}_{d_Q})]^{*}, \quad \mathbf{B}_d = [\bar{\mathbf{g}}_{0,r}(\mathbf{X}_{d_1}), \bar{\mathbf{g}}_{0,r}(\mathbf{X}_{d_2}), ..., \bar{\mathbf{g}}_{0,r}(\mathbf{X}_{d_{Q'}})]^{\dagger}$$

(5)

where $\bar{\mathbf{g}}_{0,t} = \mathbf{g}_{0,t} / \left\|\mathbf{g}_{0,t}\right\|$ and $\bar{\mathbf{g}}_{0,r} = \mathbf{g}_{0,r} / \left\|\mathbf{g}_{0,r}\right\|$ are the normalized transmit and receive background Green's function vectors at the location $\mathbf{X}_{d_q} \in C_d$ ($q = 1,...,Q$ or $q = 1,...,Q'$) , Q and Q' are the number of candidate points inside section C_d for constructing $\mathbf{A}_d$ and $\mathbf{B}_d$ respectively and $\|.\|$ denotes the vector norm. The new MSR matrices are given by

$$\hat{\mathbf{K}}_d = \mathbf{K}\mathbf{A}_d , \breve{\mathbf{K}}_d = \mathbf{B}_d \mathbf{K} \tag{6}$$

The substitution of (1) in (6) provides

$$\hat{\mathbf{K}}_d = \sum_{m=1}^{M} \sum_{m'=1}^{M} A_{m,m'} \mathbf{g}_{0,r}(\mathbf{X}_m) \mathbf{g}_{0,t}^{T}(\mathbf{X}_{m'}) \mathbf{A}_d$$

$$\breve{\mathbf{K}}_d = \sum_{m=1}^{M} \sum_{m'=1}^{M} A_{m,m'} \mathbf{B}_d \mathbf{g}_{0,r}(\mathbf{X}_m) \mathbf{g}_{0,t}^{T}(\mathbf{X}_{m'})$$

(7)

the term $\mathbf{g}_{0,t}^{T}(\mathbf{X}_{m\square})\mathbf{A}_d$ is the projection of vector $\mathbf{g}_{0,t}^{T}(\mathbf{X}_{m\square})$ on subspace $S_t^d = \text{span}\{\bar{\mathbf{g}}_{0,t}^{*}(\mathbf{X}_{d_q}), q = 1, 2, \ldots, Q\}$. Also, the term $\mathbf{B}_d\, \mathbf{g}_{0,r}(\mathbf{X}_m)$ projects vector $\mathbf{g}_{0,r}(\mathbf{X}_m)$

on subspace $S_r^d = \mathrm{span}\{\bar{\mathbf{g}}_{0,r}^{\dagger}(\mathbf{X}_{d_q}),\ q = 1, 2, \ldots, Q'\}$. If a scatterer at location $\mathbf{X}_m$ is within the section C_d or near this section, vectors $\mathbf{g}_{0,t}(\mathbf{X}_m)$ and $\mathbf{g}_{0,r}(\mathbf{X}_m)$ have noticeable projection on subspaces S_t^d and S_r^d respectively. Otherwise, these projections are negligible; specially, if $\mathbf{X}_m$ is well-separated from the points of section C_d, we have $\mathbf{g}_{0,t}(\mathbf{X}_m) \perp S_t^d$, $\mathbf{g}_{0,r}(\mathbf{X}_m) \perp S_r^d$ and $\mathbf{g}_{0,t}^T(\mathbf{X}_m)\,\mathbf{A}_d = 0$, $\mathbf{B}_d\,\mathbf{g}_{0,r}(\mathbf{X}_m) = 0$. For the ease of understanding, let M_{ws} scatterers at locations $\{\mathbf{X}_m |\ m = 1, \ldots, M_{ws},\ M_{ws} < M\}$ be inside C_d and the others be well-separated from C_d points. In absence of noise, (7) gives

$$\widehat{\mathbf{K}}_d = \sum_{m=1}^{M_{ws}} \sum_{m'=1}^{M_{ws}} A_{m,m'} \mathbf{g}_{0,r}(\mathbf{X}_m) \mathbf{g}_{0,t}^T(\mathbf{X}_{m'}) \mathbf{A}_d$$

$$\breve{\mathbf{K}}_d = \sum_{m=1}^{M_{ws}} \sum_{m'=1}^{M_{ws}} A_{m,m'} \mathbf{B}_d \mathbf{g}_{0,r}(\mathbf{X}_m) \mathbf{g}_{0,t}^T(\mathbf{X}_{m'}) \tag{8}$$

that means matrices $\widehat{\mathbf{K}}_d$ and $\breve{\mathbf{K}}_d$ contain, merely, the responses of M_{ws} scatterers, inside C_d. Because $rank\ (\widehat{\mathbf{K}}_d) = rank\ (\breve{\mathbf{K}}_d) = M_{ws}$, there are M_{ws} nonzero singular values and the use of the MUSIC with $\widehat{\mathbf{K}}_d$ and/or $\breve{\mathbf{K}}_d$ detects M_{ws} scatterers at locations $\{\mathbf{X}_m |\ m = 1, \ldots, M_{ws}\}$.

Considering the above explanation, matrices $\widehat{\mathbf{K}}_d$ and $\breve{\mathbf{K}}_d$ in (6) are focused on the scatterer responses inside section C_d (the rationale to name as the data focusing method) and the responses of other scatterers are weakened. We expect, therefore, the larger singular values correspond to the responses of scatterers within section C_d in the SVD of matrices $\widehat{\mathbf{K}}_d$ or $\breve{\mathbf{K}}_d$. The DFM, hence, weakens unwanted clutters from other sections and highlights the signature of targets inside the aimed section. In order to generate pseudo spectrum for each section, the following relation is used

$$P_{r,t}^d(\mathbf{X}) = \frac{1}{\sum_{p=M_d+1}^{N} \left|\hat{\mathbf{u}}_p^{\dagger}.\bar{\mathbf{g}}_{0,r}(\mathbf{X})\right|^2 + \sum_{p=M_d+1}^{N} \left|\check{\mathbf{v}}_p^{\dagger}.\bar{\mathbf{g}}_{0,t}^{*}(\mathbf{X})\right|^2} \tag{9}$$

where $\hat{\mathbf{u}}_p$ and $\check{\mathbf{v}}_p$ are the left and right singular vectors of $\widehat{\mathbf{K}}_d$ and $\breve{\mathbf{K}}_d$, respectively, and M_d is the dimension of signal subspace for matrices $\widehat{\mathbf{K}}_d$ or $\breve{\mathbf{K}}_d$. The normalized transmit and receive background Green vectors, i.e. $\bar{\mathbf{g}}_{0,t}$ and $\bar{\mathbf{g}}_{0,r}$, are employed so as to treat all sections similarly in terms of amplitude $P_{r,t}^d(\mathbf{X})$.

Some issues on the implementation of the DFM should be cleared. Firstly, the quantities Q and Q' are, respectively, set to the number of transmitters N_t and the number of receivers N_r in order that matrices $\widehat{\mathbf{K}}_d$ and $\breve{\mathbf{K}}_d$ have the same number of rows and columns as $\mathbf{K}$. The second issue is concerned with the shape and size of section C_d. The shape is rectangle to cover all imaging region. Regarding the size, the point spread function can be defined as [6]

$$\begin{aligned}\Gamma_r(\mathbf{X}_d,\mathbf{X}) &= \left|\overline{\mathbf{g}}^{\dagger}_{0,r}(\mathbf{X}_d)\overline{\mathbf{g}}_{0,r}(\mathbf{X})\right| \\ \Gamma_t(\mathbf{X}_d,\mathbf{X}) &= \left|\overline{\mathbf{g}}^{T}_{0,t}(\mathbf{X})\overline{\mathbf{g}}^{*}_{0,t}(\mathbf{X}_d)\right|\end{aligned} \tag{10}$$

when two points $\mathbf{X}_d$ and $\mathbf{X}$ are well-separated, $\Gamma_t(\mathbf{X}_d, \mathbf{X}) = 0$ and $\Gamma_r(\mathbf{X}_d, \mathbf{X}) = 0$ implying the two points can be well resolved. Considering L_d denotes the border around section C_d, the resolution at point $\mathbf{X}_d$ (the center of C_d) is defined as the minimum distance $\rho_d = \|\mathbf{X}_d - \mathbf{X}\|_{min}$ so that

$$\underset{\mathbf{X}\in L_d}{Max}(\Gamma(\mathbf{X}_d,\mathbf{X})) \le \xi\,\Gamma(\mathbf{X}_d,\mathbf{X}_d),\ \ 0<\xi<0.5$$

(11)

in which $\Gamma(\mathbf{X}_d, \mathbf{X})$ is equal to maximum of $\Gamma_t(\mathbf{X}_d, \mathbf{X})$ and $\Gamma_r(\mathbf{X}_d, \mathbf{X})$. For ξ = 0.5, we achieve the smallest section C^m, in which two scatters from the neighboring sections can be resolved. Therefore, the size of sections C_d should be set to the size of C^m. The generation of the pseudo spectrum with $C_d = C^m$ may cause some discontinuities at the borders of the sections. In order to make the pseudo spectrum continuous, the imaging region is divided into several sections with size C'_d, whose size is smaller than that of C^m. These sections have not overlap and cover all imaging region. The imaging region is, also, divided to several overlapping sections C_d with size of C^m so that the center of these sections and sections C'_d coincide. For each section C_d, the $\widehat{\mathbf{K}}_d$ and $\breve{\mathbf{K}}_d$ are calculated by (6); then (9) is employed to generate pseudo spectrum only for the corresponding C'_d.

The final issue is concerned with the determination of M_d in (9). Considering C_d is set to C^m, there may be just one target in a subsection C'_d and hence, M_d should be set to 1. This is the case if the focusing is perfect and matrices $\widehat{\mathbf{K}}_d$ and $\breve{\mathbf{K}}_d$ contains, only, the response of the target inside subsection C'_d. Investigation of $\Gamma(\mathbf{X}_d, \mathbf{X})$ behavior in terms of $\|\mathbf{X}\text{-}\mathbf{X}_d\|$ indicates matrices $\widehat{\mathbf{K}}_d$ and $\breve{\mathbf{K}}_d$ not only contain the response of the target inside subsection C'_d, but also include the scattering effects of the adjacent subsections or sections. In order to detect any target in C'_d under such situation, we set M_d = 2 in generating pseudo spectrum (9). It should be noted that even if the largest singular value is due to the target inside C'_d, the pseudo spectrum will have a peak at the target location with M_d = 2.

The DFM may have some failures when:

1- The signal-to-noise ratio (SNR) is low. Strong noise makes the DFM generate the noise image that hinders the image of the target.

2- The signal-to-clutter (SCR) is low for some subsections. The SCR is defined as the ratio of singular value for the point scatterer in C'_d to the largest singular value of matrices $\widehat{\mathbf{K}}_d$ or $\breve{\mathbf{K}}_d$. If the SCR is considerably low, the scattering effects of the adjacent subsections or sections dominate the response of the point scatterer in C'_d and the pseudo spectrum (9) provides false amplitude for this subsection. It should be noted that for extended targets, the resolvable point scatterers always exist in subsections C'_d, but with different scattering strength. A proper imaging is that the pseudo spectrum

(9) gives an amplitude in proportion to the scattering effect of a subsection $C_d^{'}$. Setting M_d = 2 in (9) is a compromise for proper imaging.

V. EXPERIMENTAL ASSESSMENT

The proposed method is examined using two experimental datasets provided by the Institute Fresnel, Marseille, France [11]-[12]. The pseudo spectrum amplitudes obtained from (4) and (9) are normalized to proper values so as to compare the resultant MUSIC and DFM images. The use of the estimation algorithm in [7] to evaluate *M* in (4) for the MUSIC cannot give the optimum *M* in terms of resolution. Therefore, we generate the pseudo spectrum (4) with different *M* and only present the images with the best resolution in the paper. We set M_d = 2 for the DFM in all imaging examples.

In order to quantify the level of background clutter and the spatial resolution for the images, reference

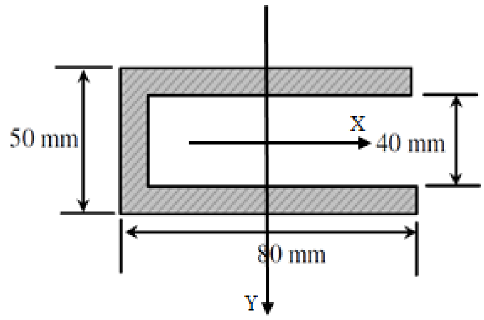

Fig. 2. Metallic target with 'U-shaped' cross section

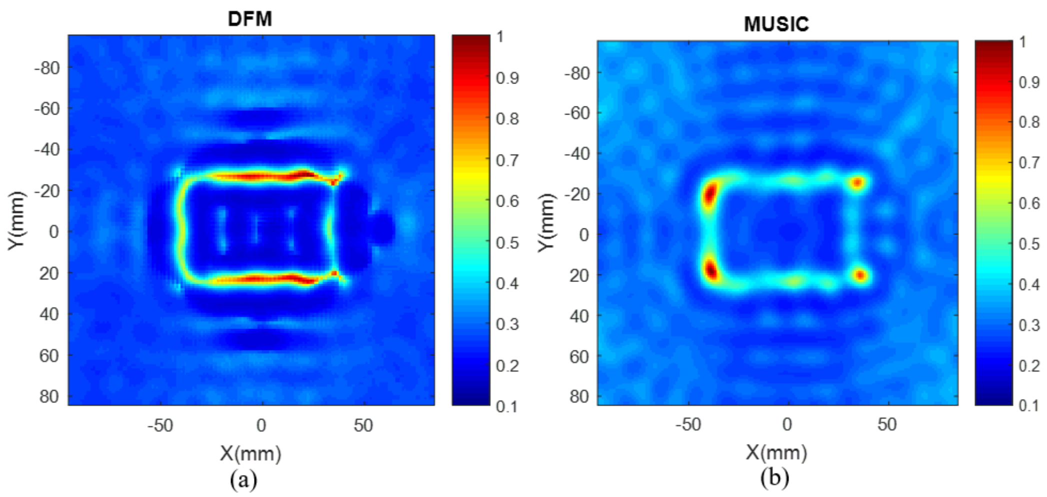

Fig. 3. Images reconstruction applied to experimental data of the geometry in Figure 2 (a) the DFM (b) the MUSIC with M = 7

[13] suggests a signal-to-mean (S/Mn) metric, which is the ratio of the target-response peak to the average of pseudo-spectrum amplitude. Because an extended target consists of many point targets, S/Mn for an extended target is determined as the ratio of the average of target-response peaks to the

average of pseudo-spectrum amplitude. The quantity S/Mn is related to the spatial resolution so that the resolution of an image becomes higher with the increase of S/Mn.

The first Fresnel measurement system in [11] employs 36 transmitters located on a circle with radius 760 mm, and 49 receivers positioned on a circular arc with radius 720 mm and angularly ranged from 60˚ to 300˚ relative to the transmitting antenna.

The first extended target that is a metallic target with 'U-shaped' cross section is shown in Fig. 2. The dimensions of the 'U-shaped' cylinder are about (80 × 50) mm^2. The frequency of reconstruction is chosen to be 10 GHz. In Fresnel data collection scenario, the activated receivers are altered for any active transmitter. Therefore, some elements in MSR matrix that correspond to inactive receivers are set to zero. The size of C^m in DFM is equal to 22mm and that of C_d' is set to 2mm. Fig. 3 illustrates image reconstruction from this experimental dataset for the MUSIC with M = 7 and the DFM with M_d = 2. It can be seen the DFM detects the borders of extended target with higher resolution. The metrics S/Mn of Fig. 3 are depicted in Table I, which shows the DFM images has better resolution than the

Table I. S/Mn metrics of Fig. 3 at 10 GHz

Algorithm	**S/Mn (dB)**
DFM	9.39
MUSIC with M=7	5.53

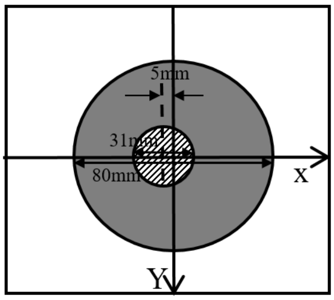

Fig. 4. Configuration of targets for the second Fresnel measurement. white = air, grey = foam and hatched = plastic

MUSIC image.

The second Fresnel measurement system in [12] employs 8 transmitters located on a circle with radius 1670 mm, and 240 receivers positioned on a circular arc with radius 1670 mm and angularly ranged from 60˚ to 300˚ relative to the transmitting antenna. The dielectric targets are shown in Fig. 4. The specifications of cylinders are as follow:

- Foam cylinder: material = SAITEC SBF 300, diameter = 80 mm, ε_r = 1.45 ± 0.15.
- Plastic cylinder: material = berylon, diameter = 31 mm, ε_r = 3 ± 0.3.

The frequency of reconstruction is chosen to be 7 GHz. The size of C^m in the DFM is equal to 24mm and that of C_d' is set to 2mm. We illustrate the results of the DFM and MUSIC reconstruction in Fig. 5. It can be seen the borders of plastic and foam cylinders are detected in the DFM, whereas the MUSIC is not able to detect the location of targets because the number of transmitter antennas is low in this measurement.

VI. CONCLUSION

We introduce a data focusing method that can be used for microwave imaging. The DFM reduces the response power of the scatterers outside the section of interest; but, it keeps the scatterer responses from inside of the section. As a result, the strengths of singular values for the targets inside the intended section is enhanced several units against the others. Such an enhancement makes the requirement for the MUSIC algorithm in terms of the number of transmitter-receiver antennas be satisfied for extended targets.

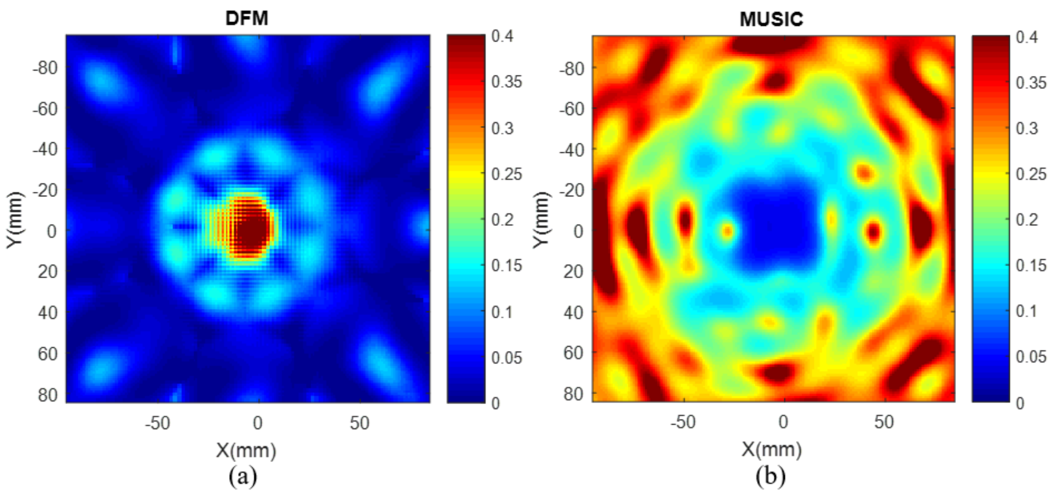

Fig. 5. Images reconstruction for the experimental data of the geometry in Figure 4 (a) the DFM (b) the MUSIC with M=4

We apply the DFM and the conventional MUSIC to the real experimental data to demonstrate the merits of our method. The results indicate the DFM provides better image than the MUSIC for extended targets even if the optimized MUSIC is employed.

ACKNOWLEDGMENT

We would appreciate the Institute Fresnel, Marseille, France for providing the experimental data.

REFRENCES

[1] K. Agarwal and X. Chen, "Applicability of MUSIC-type imaging in two-dimensional electromagnetic inverse problems," *IEEE Trans. Antennas Propag.*, vol. 56, no. 10, pp. 3217-3223, Oct. 2008.

[2] R. Fazli, M. Nakhkash, and A.A. Heidari, "Alleviating the practical restrictions for MUSIC algorithm in actual microwave imaging systems: experimental assessment," *IEEE Trans. Antennas Propag.*, vol. 62, no. 6, pp. 3108-3118, June 2014.

[3] M.H. Bah, J.S. Hong, D.A. Jamro, "UWB patch antenna and breast mimicking phantom design and implementation for microwave breast cancer detection using Time Reversal MUSIC," Microwave *and Optical Technology Letters.*, vol. 58, no. 3, pp. 549-554, March 2016.

[4] X. Chen and Y. Zhong, "MUSIC electromagnetic imaging with enhanced resolution for small inclusions," *Inverse Prob.*, vol. 25, no. 1, 2009.

[5] W.K. Park, "Multi-frequency MUSIC for searching small dielectric inclusions surrounded by random scatterers," Progress in Electromagnetic Research Symposium (PIERS)., Shanghai, China, 2016.

[6] S. Hou, K. Solna, and H. Zhao, "A direct imaging algorithm for extended targets," *Inverse Prob.*, vol. 22, pp. 1151-1178, 2006.

[7] E.A. Marengo, F.K. Gruber, F. Simonetti, "Time-Reversal MUSIC Imaging of Extended Targets," *IEEE Trans. Image Processing*., vol. 16, no. 8, pp. 1967-1984, August 2007.

[8] L.O. Foldy, "The multiple scattering of waves," *Phys. Rev.*, vol. 67, no. 3-4, pp. 107-119, 1945.

[9] M. Lax, "Multiple scattering of waves," *Rev. Mod. Phys.*, vol. 23, no. 4, pp. 287-310, Oct.-Dec. 1951.

[10] E.A. Marengo, "Single-snapshot signal subspace methods for active target location: part I: multiple scattering case," Int. Conf. IASTED, Banff, Canada, pp. 161-166, 2005.

[11] K. Belkebir and M. Saillard, "Testing inversion algorithms against experimental data," *Inverse Prob.*, vol. 17, no. 6, pp. 1565-1571, 2001.

[12] J.M. Geffrin, P. Sabouroux and C. Eyraud, "Free space experimental scattering database continuation: experimental set-up and measurement precision," *Inverse Problems, vol. 21, no. 6*, pp. 117–130, 2005.

[13] D. Byrne, I.J. Craddock, "Time-Domain Wideband Adaptive Beam forming for Radar Breast Imaging," *IEEE Trans. Antennas Propag.*, vol. 63, no. 4, pp. 1725 – 1735, April 2015.